

Effect of Ligand Structure on Activation Rate Constants in ATRP

Wei Tang and Krzysztof Matyjaszewski*

Center for Macromolecular Engineering, Department of Chemistry, Carnegie Mellon University, 4400 Fifth Avenue, Pittsburgh, Pennsylvania 15213

Received May 1, 2006; Revised Manuscript Received May 18, 2006

ABSTRACT: Activation rate constants (k_{act}) for Cu complexes with various nitrogen-based ligands for Cu-mediated ATRP were determined at 35 °C in acetonitrile. The ratio of k_{act} for complexes with different ligands exceeds 1 million times. The general order of Cu complex activity for ligands is tetradentate (cyclic-bridged) > tetradentate (branched) > tetradentate (cyclic) > tetradentate (linear) > tridentate > bidentate ligands. The nature of nitrogen atoms in ligands also plays a significant role in the activity of the Cu complexes and follows the order pyridine \geq aliphatic amine > imine.

Introduction

Atom transfer radical polymerization mediated by Cu complexes (ATRP, Scheme 1) is a powerful and robust controlled radical polymerization technique useful for preparation of many well-defined polymers with precisely controlled architecture.^{1–12} The control in ATRP depends largely on an appropriate equilibrium between the activation process (generation of radicals, k_{act}) and the deactivation process (formation of alkyl halides, k_{deact}). The equilibrium between the two processes ($K_{\text{ATRP}} = k_{\text{act}}/k_{\text{deact}}$) determines the concentration of radicals and subsequently the rates of polymerization and termination as well as polydispersities, as shown in eqs 1 and 2.⁶ Usually K_{ATRP} is very small in order to maintain a low radical concentration and to minimize termination reactions. At the same time, each rate constant (k_{act} and k_{deact}) affects the level of control in the polymerization. Ideally, both k_{act} and k_{deact} should be large enough (though $k_{\text{act}} \ll k_{\text{deact}}$) to provide good control over the polymerization while providing a reasonable polymerization rate.

$$\ln \frac{[M]_0}{[M]_t} = \frac{k_p k_{\text{act}} [P_m - X][Cu^I]}{k_{\text{deact}} [X - Cu^{II}]} \quad (1)$$

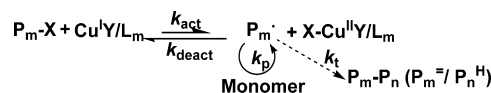
$$\frac{M_w}{M_n} = 1 + \left(\frac{k_p [R - X]_0}{k_{\text{deact}} [X - Cu^{II}]} \right) \left(\frac{2}{p} - 1 \right) \quad (2)$$

The evaluation of the reaction parameters such as k_{act} and k_{deact} is crucial for further understanding of ATRP. Studies have thus far concentrated on measuring k_{act} for polymeric and monomeric systems using spectroscopy and chromatography.^{13–33} However, most of the values were obtained under different reaction conditions using various techniques and methods. To better compare and understand the kinetics of ATRP, we present here the effect of ligand structure on the activation process by determining the k_{act} under similar reaction conditions and using the same methodology.

Experimental Section

Materials. Ethyl 2-bromoisobutyrate (EtBrIB, 99%, Aldrich), methyl 2-chloropropionate (MCIP, 97%, Aldrich), methyl chloroacetate (MCIAC, 99+%, Aldrich), benzyl bromide (BzBr, 98%, Aldrich), 1,2,4-trichlorobenzene (TCB, 99%, Aldrich), and 2,2,6,6-

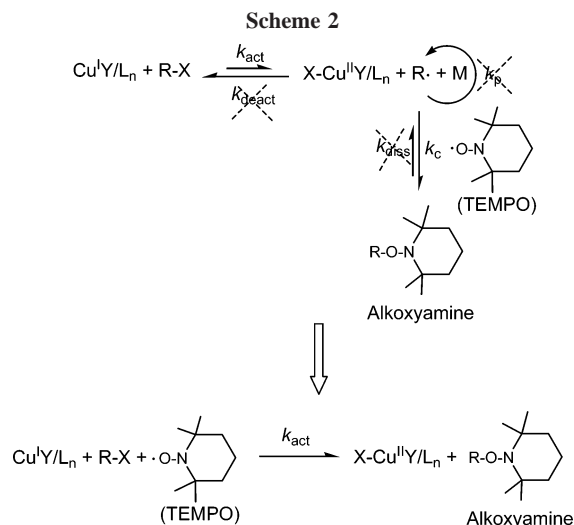
Scheme 1. Proposed Mechanism for ATRP



tetramethylpiperidiny-1-oxy (TEMPO, 99%, Aldrich) were used as received. *N*-(*n*-Propyl)pyridylmethanimine (NPPMI) and *N*-(*n*-octyl)pyridylmethanimine (NOPMI) were synthesized by condensation of *n*-propylamine and *n*-octylamine, with pyridine-2-carboxaldehyde, respectively.³⁴ Tris(2-(dimethylamino)ethyl)amine (Me₆TREN) was synthesized by methylation of tris(2-aminoethyl)amine (TREN).³⁵ Tris(2-(diethylamino)ethyl)amine (Et₆TREN) was synthesized according to the literature.³⁶ Tris(2-(di(2-cyanoethyl)amino)ethyl)amine (AN₆TREN), tris(2-(di(2-(methoxycarbonyl)ethyl)amino)ethyl)amine (MA₆TREN), and tris(2-(di(2-(*n*-butoxycarbonyl)ethyl)amino)ethyl)amine (BA₆TREN) were synthesized by Michael addition of TREN with acrylonitrile, methyl acrylate, and *n*-butyl acrylate, respectively.³⁷ 2,5,9,12-Tetramethyl-2,5,9,12-tetraazatridecane (N[2,3,2]),³⁸ 2,6,9,13-tetramethyl-2,6,9,13-tetraazatetradecane (N[3,2,3]),³⁸ 4,11-dimethyl-1,4,8,11-tetraazabicyclo[6.6.2]hexadecane (Cyclam-B),³⁹ *N,N'*-dimethyl-*N,N'*-bis((pyridin-2-yl)methyl)ethane-1,2-diamine (BPED),⁴⁰ 4,4'-di(9-heptadecyl)-2,2'-bipyridine (dHDbpy),⁴¹ 4,4'-di(5-nonyl)-2,2'-bipyridine (dNbpy),⁴² 4,4',4''-tris(5-nonyl)-2,2':6',2''-terpyridine (tNtpy),⁴³ *N,N*-bis(2-pyridylmethyl)octadecylamine (BPMODA),⁴⁴ and tris[(2-pyridyl)methyl]amine (TPMA)⁴⁴ were synthesized according to the literature. 2,5,8,12-Tetramethyl-2,5,8,12-tetraazatridecane (N[2,2,3]) was synthesized by similar methylation of 2,5,8,12-tetraazatridecane tetrahydrochloride salt with formaldehyde and formic acid and distilled under reduced pressure. *N,N,N',N'*-Tetra[(2-pyridyl)methyl]ethylenediamine (TPEDA) was synthesized by a reaction of benzyl chloride and ethylenediamine.^{45,46} *N*-[2-(Dimethylamino)ethyl]-*N,N'*-trimethyl-1,3-propanediamine (N[2,3]) was synthesized by methylation of *N*-(2-aminoethyl)-1,3-propanediamine. 2,2'-Bipyridine (bpy, 99%, Aldrich), *N,N,N',N'*-tetramethylethylenediamine (TMEDA, 99%, Aldrich), 1,4,7-trimethyl-1,4,7-triazonane (Me₃TAN, Aldrich), 1,4,8,11-tetramethyl-1,4,8,11-tetraazacyclotetradecane (Me₄Cyclam), *N,N,N',N',N'*-pentamethyldiethylenetriamine (PMDETA, 99%, Aldrich), and 1,1,4,7,10,10-hexamethyltriethylenetetramine (HMTETA, 97%, Aldrich) were used as received. All the other reagents and solvents were used as received.

Typical Procedure for Measurement of Activation Rate Constant (Cu^{II}Br/PMDETA with EtBrIB). Stock solutions of EtBrIB (4×10^{-3} M) were prepared by adding 7.8 mg (0.04 mmol) of the corresponding reactant along with 14.5 mg (0.08 mmol) of internal standard, TCB, and 62.5 mg (0.4 mmol) of TEMPO in MeCN in a 10 mL volumetric flask. Similarly, a 0.08 M stock solution of PMDETA was prepared in MeCN. In a Schlenk flask,

* Corresponding author: e-mail km3b@andrew.cmu.edu; fax 412-268-6897.



11.5 mg (0.08 mmol) of $\text{Cu}^{\text{I}}\text{Br}$ was taken, and the flask was degassed and backfilled with N_2 three times. 1 mL stock solution of PMDETA along with 2 mL of acetonitrile was subjected to freeze–pump–thaw cycle three times and then transferred to the Schlenk flask through a N_2 -purged syringe. Then, 1 mL of the stock solution of EtBrIB, TCB, and TEMPO was degassed by three freeze–pump–thaw cycles and transferred to the Schlenk flask through a N_2 -purged syringe. The flask was stirred, and a sample was taken immediately for the gas chromatography (GC) analysis generating the data for time zero. The reaction was carried out at 35 °C under constant stirring. Samples were taken at timed intervals, and the consumption of EtBrIB with time was monitored by GC. GC was performed using a Shimadzu GC-17A, AOC-20i autosampler, and J&W Scientific DB 608 column (30 m \times 0.53 mm) with a (electron capture detector) (ECD) detector. The ECD detector is very sensitive to alkyl halides and governed by radiation (β -ray) from a ^{63}Ni source sealed in the ECD cell ionized by an inert gas (N_2).

Simulation. The Predici program (version 6.3.1) was used for all kinetic modeling.⁴⁷ It employs an adaptive Rothe method as a numerical strategy for time discretization. The concentrations of all species can be followed with time.

Method. The activation rate constants were determined using the trapping experiments that are also the basis for determining the dissociation rate parameters of alkoxyamines.⁴⁸ The radicals originating from homolytic halogen abstraction from the alkyl halides are irreversibly trapped by a stable nitroxide radical, 2,2,6,6-tetramethylpiperidinyl-1-oxyl (TEMPO), to yield the corresponding alkoxyamines (Scheme 1).²⁰ To obtain irreversible kinetics, the radicals originating from the alkyl halides should be immediately trapped by TEMPO with no transformation back to the dormant species. This was achieved by using a large excess of TEMPO (~ 10 -fold) with respect to alkyl halides. This process is also facilitated due to a higher rate constant for radical coupling than deactivation ($k_c \gg k_{\text{deact}}$).²⁰ An excess of Cu^{I} (20 times with respect to alkyl halide) was used to make the kinetic analysis straightforward, i.e., to provide pseudo-first-order kinetic conditions. From the slope of the pseudo-first-order plots the activation rate constants (k_{act}) were determined (eq 3).

$$\text{pseudo-first-order: } [\text{Cu}^{\text{I}}\text{Y/L}_n]_0 \gg [\text{R-X}]_0$$

$$-\frac{d \ln[\text{R-X}]}{dt} = \text{slope} = k_{\text{act}}[\text{Cu}^{\text{I}}\text{Y/L}_n]_{\text{act}} \quad (3)$$

where $[\text{Cu}^{\text{I}}\text{Y/L}_n]_{\text{act}}$ is the active concentration in the reaction solution.

To verify the validity of the proposed method for determination of the k_{act} for ATRP, a simple simulation was carried out using the Predici program. A kinetic plot is shown in Figure 1. From the

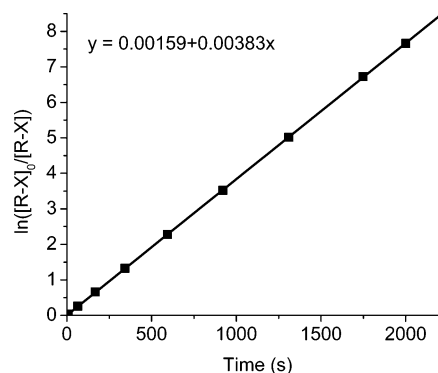


Figure 1. Simulation for the pseudo-first-order determination of k_{act} for ATRP. $[\text{R-X}]_0 = 1 \times 10^{-3} \text{ M}$, $[\text{Cu}^{\text{I}}\text{Y/L}_n]_0 = 0.02 \text{ M}$, $[\text{TEPMPO}]_0 = 0.01 \text{ M}$, $k_{\text{act}} = 0.2 \text{ M}^{-1} \text{ s}^{-1}$, $k_{\text{deact}} = 2.0 \times 10^7 \text{ M}^{-1} \text{ s}^{-1}$, $k_c = 1.3 \times 10^8 \text{ M}^{-1} \text{ s}^{-1}$, $k_{\text{diss}} = 2.8 \times 10^{-6} \text{ M}^{-1} \text{ s}^{-1}$.²⁰

plot slope one can calculate k_{act} using eq 3, i.e., $k_{\text{act}} = 0.192 \text{ M}^{-1} \text{ s}^{-1}$, which is very close to the value used in the simulation ($0.2 \text{ M}^{-1} \text{ s}^{-1}$). It should be noted that most values of k_{deact} are around or less than the value used in simulation ($2.0 \times 10^7 \text{ M}^{-1} \text{ s}^{-1}$).^{20,49} Therefore, it is appropriate to use the proposed method to determine k_{act} for ATRP.

Results and Discussion

The activation rate constants were obtained through pseudo-first-order kinetics by using a radical trapping agent, TEMPO, in MeCN at 35 °C. Consumption of the initiator was monitored by GC using ECD detector, which is particularly sensitive to halogen-containing compounds. Several nitrogen-based ligands have been investigated for Cu-mediated ATRP.^{34–36,42–44,50–54} In the current study, to compare the activity of these Cu complexes with ligands in the activation process, most of the experiments were performed under similar conditions, i.e., in the same solvent (MeCN), at the same temperature (35 °C), and with the same initiator (EtBrIB). Because reaction rates with some ligands were too fast to be measured by GC using EtBrIB as the initiator, less active alkyl halides such as BzBr (or MBrP or MCIP) were used. The extrapolated values are thus calculated, assuming that EtBrIB and BzBr have the same selectivity toward Cu^{I} complexes with more active ligands as with less active ligands. For example, k_{act} for $\text{Cu}^{\text{I}}\text{Br}/\text{PMDETA}$ with EtBrIB was $2.70 \text{ M}^{-1} \text{ s}^{-1}$ and with BzBr was $0.10 \text{ M}^{-1} \text{ s}^{-1}$. For $\text{Cu}^{\text{I}}\text{Br}/\text{Me}_3\text{TAN}$ with EtBrIB k_{act} was $0.38 \text{ M}^{-1} \text{ s}^{-1}$ and with BzBr is $0.012 \text{ M}^{-1} \text{ s}^{-1}$. These values gave a relative ratio of $k_{\text{act}} = 27$ and 32, respectively. More extensive results of selectivity studies will be reported separately.

The role of the ligand in ATRP is to solubilize the Cu salts and to tune the Cu catalyst activity. The choice of ligand greatly influences the effectiveness of the catalyst. The redox potential of the Cu complex serves as a useful guideline for catalyst design. A linear correlation between the redox potential of the Cu complexes and the logarithmic k_{act} , k_{deact} , and $k_{\text{act}}/k_{\text{deact}}$ was reported for tridentate ligands with PEBr.¹⁸ Nitrogen-based ligands generally work well for Cu-mediated ATRP. In contrast, sulfur, oxygen, or phosphorus ligands are less effective due to the different electronic effects or unfavorable binding constants.^{40,55} Cu complexes formed with monodentate nitrogen-based ligands do not promote successful ATRP; therefore, multidentate ligands were investigated in this study.

Bidentate Ligands (N2). Bidentate ligands were among the least active complexes investigated in this study. These ligands include *N*-alkyl-(2-pyridyl)methanimine (PMI) ligands (NPPMI and NOPMI), 2,2'-bipyridine-based ligands (bpy, dHdbpy, and dNbpy), and TMEDA, as listed in Table 1.

Table 1. Activation Rate Constants for Bidentate Ligands^a

Structure	Name	k_{act} ($\text{M}^{-1}\text{s}^{-1}$)	Relative Ratio
	NPPMI (R = <i>n</i> -Pr) NOPMI (R = <i>n</i> -Oct)	2.4×10^{-3}	1
	TMEDA	0.042	~20
	bpy	0.066	~30
	dHDbpy	0.20	~80
	dNbpy	0.60	250

^a Values of k_{act} were measured using $[\text{EtBrIB}]_0 = 1 \text{ mM}$ and $[\text{Cu}^{\text{I}}\text{Br/L}]_0 = 20 \text{ mM}$, at 35°C in MeCN.

PMI ligands³⁴ and bpy^{53,56} are commonly used in ATRP, leading to well-controlled polymerizations but to relatively slow polymerization rates. The incorporation of long alkyl groups onto pyridine rings makes the bpy ligands (dHDbpy and dNbpy) more soluble in less polar solvents and also increases complexes activity (3 and 6 times in comparison with bpy, respectively). Compared with bpy, TMEDA forms complexes ~4 times less active and gives less controlled polymerization of styrene, MA, and MMA with relatively high polydispersities and slow polymerization.⁵⁴ With these ligands, polymers with very low polydispersities were formed. This was attributed to the increased rate of deactivation of the growing radicals in solution due to better solubility of deactivators.⁴²

Tridentate Ligands (N3). Four tridentate ligands were investigated, i.e., PMDETA (or N[2,2]), N[2,3], BPMODA, and tNtpy (Table 2).

The structure of N[2,3] is quite similar to PMDETA except that N[2,3] has one propylene linkage and one ethylene linkage. However, $\text{Cu}^{\text{I}}\text{Br}/\text{N}[2,3]$ is ~300 times less active than $\text{Cu}^{\text{I}}\text{Br}/\text{PMDETA}$. This is in agreement with earlier reports that an ethylene linkage between the coordinating nitrogens is better than a propylene linkage for coordination angle, and ligands with linkages longer than three carbons yield polymerization rate similar to that with monodentate ligands.⁴⁰ BPMODA has a structure similar to PMDETA and forms a complex which is only ~2 times less active than one with PMDETA. PMDETA is one of the most commonly used ligands in ATRP due to its commercially availability and relatively low cost. The value of k_{act} for $\text{Cu}^{\text{I}}\text{Br}/\text{PMDETA}$ is in good agreement with previously reported values using GC and stopped-flow techniques.^{26,28} Activity of complexes with tNtpy is larger than that with PMDETA. It should be noted that tNtpy is only soluble in nonpolar solvents such as toluene but is insoluble in MeCN. The value of k_{act} for tNtpy in MeCN was thus estimated from that in toluene by assuming that k_{act} is ~2 times larger in MeCN than in toluene.³¹ It seems that pyridine based ligands generate more active catalyst than those with aliphatic amines.

Linear Tetradentate Ligands (N4-Linear). Activation rate constants with complexes with five linear tetradentate ligands were studied (Table 3). Four of these linear tetradentate ligands

Table 2. Activation Rate Constants for Tridentate Ligands^a

Structure	Name	k_{act} ($\text{M}^{-1}\text{s}^{-1}$)	Relative ratio
	N[2,3]	9.2×10^{-3}	1
	BPMODA	1.1	~120
	PMDETA (N[2,2])	2.7	~300
	tNtpy	8.2*	~900

^a Values of k_{act} were measured using $[\text{EtBrIB}]_0 = 1 \text{ mM}$ and $[\text{Cu}^{\text{I}}\text{Br/L}]_0 = 20 \text{ mM}$, at 35°C in MeCN. *Value was extrapolated from the k_{act} for $\text{Cu}^{\text{I}}\text{Br}/\text{tNtpy}$ with EtBrIB in toluene (the complex of $\text{Cu}^{\text{I}}\text{Br}/\text{tNtpy}$ is not soluble in MeCN) in 4 times diluted solution, by assuming that the k_{act} is 2 times lower in toluene than in MeCN.³¹

Table 3. Activation Rate Constants for Linear Tetradentate Ligands^a

Structure	Name	k_{act} ($\text{M}^{-1}\text{s}^{-1}$)	Relative ratio
	N[2,3,2]	1.2×10^{-3}	1
	N[3,2,3]	5.0×10^{-3}	4
	HMTETA (N[2,2,2])	0.14	~120
	N[2,2,3]	0.23	~190
	BPED	4.5*	3750

^a Values of k_{act} were measured using $[\text{EtBrIB}]_0 = 1 \text{ mM}$ and $[\text{Cu}^{\text{I}}\text{Br/L}]_0 = 20 \text{ mM}$, at 35°C in MeCN. *Value was extrapolated from the k_{act} for $\text{Cu}^{\text{I}}\text{Cl}/\text{BPED}$ with MCIP, i.e., $k_{\text{act}}(\text{Cu}^{\text{I}}\text{Br}/\text{BPED with EtBrIB}) = k_{\text{act}}(\text{Cu}^{\text{I}}\text{Cl}/\text{BPED with MCIP}) \times k_{\text{act}}(\text{Cu}^{\text{I}}\text{Br}/\text{PMDETA with EtBrIB}) / (k_{\text{act}}(\text{Cu}^{\text{I}}\text{Cl}/\text{PMDETA with MCIP}) = 0.025 \times 2.7/0.015 \text{ M}^{-1} \text{ s}^{-1} = 4.5 \text{ M}^{-1} \text{ s}^{-1}$.

are aliphatic amines. The only difference among N[2,2,2] (or HMTETA), N[2,2,3], N[2,3,2], and N[3,2,3] is the number and the position of the propylene linkage between nitrogen atoms. N[2,2,2] and N[2,2,3] form relatively active complexes which lead to controlled polymerization.⁵⁴ However, N[2,3,2] and N[3,2,3] form much less active complexes. Apparently, ligands

Table 4. Activation Rate Constants for Branched Tetradentate Ligands^c

Structure	Name	k_{act} ($\text{M}^{-1}\text{s}^{-1}$)	Relative ratio
	AN ₆ TREN	0.012	1
	Et ₆ TREN	0.044	~4
	MA ₆ TREN	1.2	100
	BA ₆ TREN	4.1 ^a	~340
	TPMA	62 ^b	~5200
	Me ₆ TREN	4.5×10^2 ^b	37,500

^a Value was extrapolated from the k_{act} for Cu^IBr/BA₆TREN with MBrP, i.e., k_{act} (Cu^IBr/BA₆TREN with EtBrIB) = k_{act} (Cu^IBr/BA₆TREN with MBrP) \times k_{act} (Cu^IBr/PMDETA with EtBrIB)/(Cu^IBr/PMDETA with MBrP) = $0.50 \times 2.7/0.33 \text{ M}^{-1} \text{ s}^{-1} = 4.1 \text{ M}^{-1} \text{ s}^{-1}$. ^b Values were extrapolated from the k_{act} for Cu^IBr/TPMA (Me₆TREN) with MClAc, i.e., k_{act} (Cu^IBr/TPMA with EtBrIB) = k_{act} (Cu^ICl/TPMA with MClAc) \times k_{act} (Cu^IBr/PMDETA with EtBrIB)/(Cu^ICl/PMDETA with MClAc) = $0.037 \times 2.7/1.6 \times 10^{-3} \text{ M}^{-1} \text{ s}^{-1} = 62 \text{ M}^{-1} \text{ s}^{-1}$ and k_{act} (Cu^IBr/Me₆TREN with EtBrIB) = k_{act} (Cu^ICl/Me₆TREN with MClAc) \times k_{act} (Cu^IBr/PMDETA with EtBrIB)/(Cu^ICl/PMDETA with MClAc) = $0.27 \times 2.7/1.6 \times 10^{-3} \text{ M}^{-1} \text{ s}^{-1} = 4.5 \times 10^2 \text{ M}^{-1} \text{ s}^{-1}$. ^c Values of k_{act} were measured using [EtBrIB]₀ = 1 mM and [Cu^IBr/L]₀ = 20 mM, at 35 °C in MeCN.

with a central propylene linkage or two side propylene linkage reduce complex activity. However, a complex with ligands containing only one side propylene linkage is more active than the HMTETA complex. This can be ascribed to higher complex flexibility and faster transformation from the Cu^I to Cu^{II} state.

BPED is a mixed pyridine–amine tetradentate ligand, which forms complexes with ~30 times higher activity than N[2,2,2].

Table 5. Activation Rate Constants for Hexadentate Ligands^a

Structure	Name	k_{act} ($\text{M}^{-1}\text{s}^{-1}$)	Relative ratio
	TPEDA	10.8 [*]	/

^a Values of k_{act} were measured using [EtBrIB]₀ = 1 mM and [Cu^IBr/L]₀ = 20 mM, at 35 °C in MeCN. *Value was extrapolated from the k_{act} for Cu^IBr/TPEDA with MBrP, i.e., k_{act} (Cu^IBr/TPEDA with EtBrIB) = k_{act} (Cu^IBr/TPEDA with MBrP) \times k_{act} (Cu^IBr/PMDETA with EtBrIB)/(Cu^IBr/PMDETA with MBrP) = $1.28 \times 2.7/0.33 \text{ M}^{-1} \text{ s}^{-1} = 10.5 \text{ M}^{-1} \text{ s}^{-1}$.

Table 6. Activation Rate Constants for Cyclic Ligands^a

Structure	Name	k_{act} ($\text{M}^{-1}\text{s}^{-1}$)	Relative ratio
	Me ₃ TAN	0.38	1
	Me ₄ Cyclam	0.67	~2
	Cyclam-B	7.1×10^2 [*]	~1800

^a Values of k_{act} were measured using [EtBrIB]₀ = 1 mM and [Cu^IBr/L]₀ = 20 mM, at 35 °C in MeCN. *Value was extrapolated from the k_{act} for Cu^IBr/Cyclam-B with MClAc, i.e., k_{act} (Cu^IBr/Cyclam-B with EtBrIB) = k_{act} (Cu^ICl/Cyclam-B with MClAc) \times k_{act} (Cu^IBr/PMDETA with EtBrIB)/(Cu^ICl/PMDETA with MClAc) = $0.42 \times 2.7/1.6 \times 10^{-3} \text{ M}^{-1} \text{ s}^{-1} = 4.5 \times 10^2 \text{ M}^{-1} \text{ s}^{-1}$.

The value of k_{act} for BPED with EtBrIB was extrapolated from that of Cu^IBr/BPED with MClP. The high activity of Cu^IBr/BPED suggests that pyridine-containing ligands could generate more active catalyst than those with aliphatic amines.

Branched Tetradentate Ligands (N4-Branched). There are six branched tetradentate ligands listed in Table 4. Some branched tetradentate ligands form very active Cu complexes. The k_{act} for Cu^IBr/BA₆TREN with EtBrIB was extrapolated from that with MBrP, and the k_{act} for Cu^IBr/TPMA and Cu^IBr/Me₆TREN with EtBrIB were extrapolated from those with MClAc. Direct measurement of the k_{act} Cu^IBr/Me₆TREN with EtBrIB was carried out by stopped-flow technique, giving a value of $7.7 \times 10^3 \text{ M}^{-1} \text{ s}^{-1}$ at 25 °C,²⁸ which is ~17 times larger than the extrapolated value. Thus, the assumption that EtBrIB and MClAc have the same selectivity toward Cu^IBr/Me₆TREN and Cu^ICl/PMDETA may not be fully correct. In an independent project we will study the effect of complex structure on relative activities of alkyl halides. Nevertheless, for consistency and comparison with other ligands, we use here the extrapolated values.

Me₆TREN forms one of the most active complexes among all the ligands studied and was particularly successful for ATRP of MA at ambient temperature.⁵⁷ However, the substitution of methyl groups by ethyl groups in Me₆TREN leads to Et₆TREN with ~10 000 times lower activity for the Cu complexes.³⁶ The incorporation of cyano groups makes Cu^IBr/AN₆TREN even ~4 times less active than Cu^IBr/Et₆TREN. The cyano groups

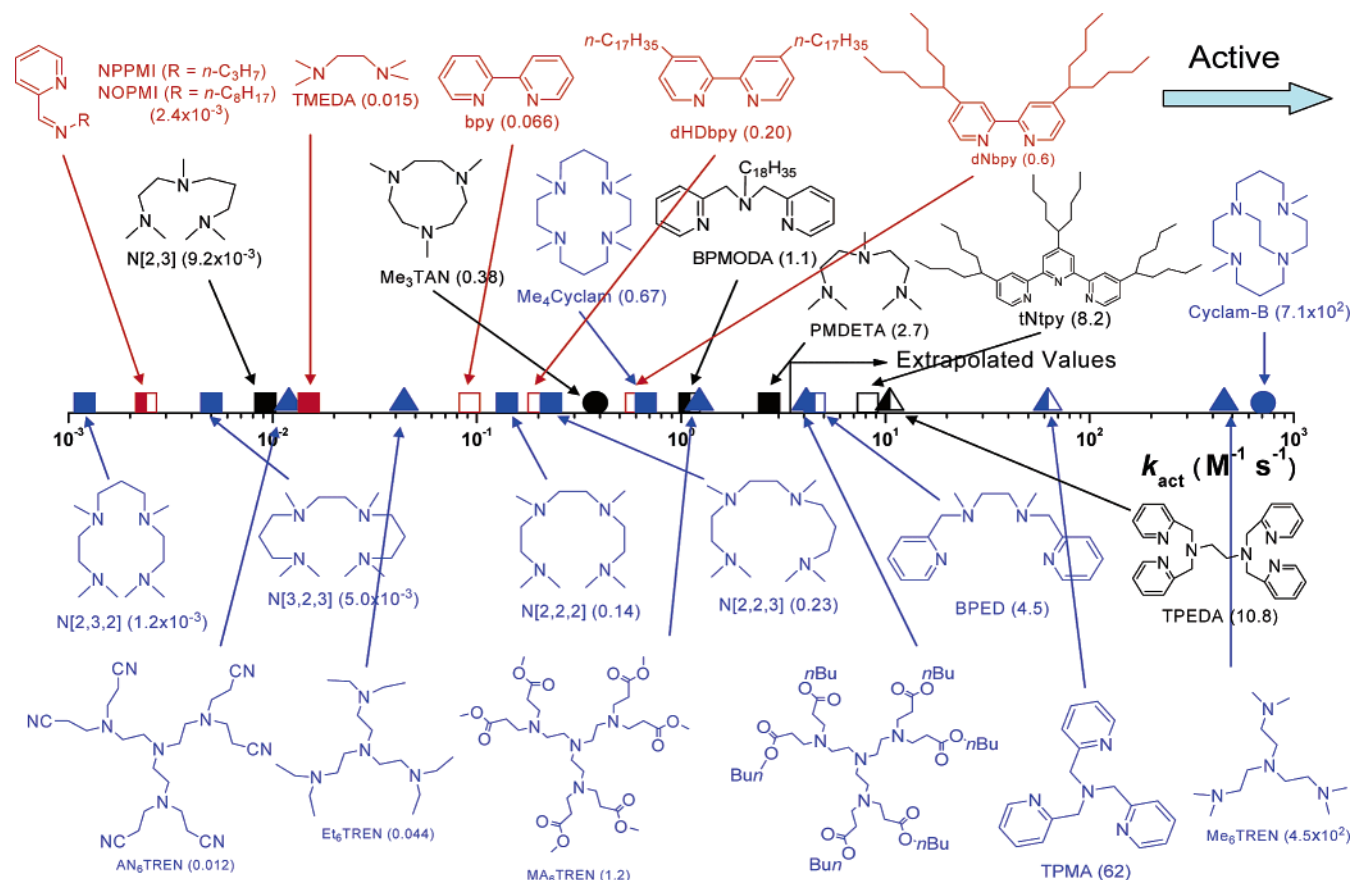


Figure 2. ATRP activation rate constants for various ligands with EtBrIB in the presence of Cu^IY (Y = Br or Cl) in MeCN at 35 °C: N2, red; N3, black; N4, blue; amine/imine, solid; pyridine, open. Mixed, left-half solid; linear, □; branched, ▲; cyclic, ○.

might contribute to the coordination of the ligand to Cu^I , and the $\text{Cu}^I\text{Br}/\text{AN}_6\text{TREN}$ could not accommodate another bromine atom to form a Cu^{II} complex. TPMA is also a branched tetradentate ligand with pyridine substituents, with a similar structure to Me_6TREN . TPMA is especially good ligand for aqueous polymerization since its Cu^I complex does not disproportionate in aqueous media.⁵⁸ $\text{Cu}^I\text{Br}/\text{TPMA}$, however, is ~ 7 times less active than $\text{Cu}^I\text{Br}/\text{Me}_6\text{TREN}$. The effect of the nature of nitrogen in the ligands will be discussed in detail later (Table 7).

Hexadentate Ligand. The ligand TPEDA which was reported by Shen^{45,46} is the only hexadentate ligand that was studied (Table 5). The Cu^I complex formed by this ligand is fairly active (4 times more active than $\text{Cu}^I\text{Br}/\text{PMDETA}$ and ~ 2 times more active than $\text{Cu}^I\text{Br}/\text{BPED}$).

Cyclic Ligands (N-Cyclic). Complexes with three cyclic ligands were studied: Me_4Cyclam , Cyclam-B, and Me_3TAN (Table 6). A Cu^I complex with Me_4Cyclam as the ligand gives very fast polymerization and could be applied to vinyl acetate and acrylamides.^{52,59} However, it has a $k_{act} = 0.67 \text{ M}^{-1} \text{ s}^{-1}$, i.e., much smaller than the $\text{Cu}^I\text{Br}/\text{Me}_6\text{TREN}$ complex. This is possibly because its deactivation rate constant is very small, which leads to a fast polymerization according to eq 1. The incorporation of an ethylene bridge into Me_4Cyclam to connect two of the diagonal nitrogen atoms makes the Cu^I complex with the ligand (Cyclam-B) extremely active. It is ~ 1000 times more active than $\text{Cu}^I\text{Br}/\text{Me}_4\text{Cyclam}$, and it is the most active ligand we have studied so far. Me_3TAN is a tridentate ligand and was reported to be a good ligand for some transition metal complexes; however, it forms a Cu^IBr complex with an average activity possibly due to its relative small ring size.⁶⁰

Pyridine vs Amine Ligands. Structurally similar pyridine and amine ligands are listed in Table 7. Cu complexes with

bidentate, tridentate, and linear tetradentate pyridine ligands are more active than those with corresponding structurally similar aliphatic amine ligands (e.g., bpy vs TMEDA, tNtpy vs PMDETA and BPED vs HMTETA). However, branched tetradentate pyridine ligand forms a complex with a little lower activity than the corresponding aliphatic amine (e.g., TPMA vs Me_6TREN). $\text{Cu}^I\text{Br}/\text{PMI}$ complexes are even less active (~ 30 times) than $\text{Cu}^I\text{Br}/\text{TMEDA}$.

Comparison of All Ligands. Figure 2 presents all values of k_{act} with EtBrIB (measured directly or extrapolated) arranged in a logarithmic scale for a better comparison of activities of Cu complexes with ligands discussed above. Extrapolated values may underestimate the values of k_{act} for active complexes. As discussed above, $\text{Cu}^I\text{Br}/\text{Me}_6\text{TREN}$ and plausibly also $\text{Cu}^I\text{Br}/\text{Cyclam-B}$ might have values of k_{act} larger than $10^4 \text{ M}^{-1} \text{ s}^{-1}$ as determined directly by stopped-flow technique.²⁸ However, with limited availability of the k_{act} from stopped-flow technique, the extrapolated values were used for a consistent comparison between the complexes. The extrapolated values should still maintain the order of activities of complexes.

The ratios of activity for complexes with different ligands exceeds 1 million times. The catalysts become more active when its Cu^{II} state is better stabilized by the ligand, according to electrochemical studies.^{20,55,61,62} Tetradentate ligands form the most active complexes, especially Cyclam-B, in which the ethylene linkage further stabilizes the Cu^{II} complex. Complexes with branched tetradentate ligands produce the most active catalysts; e.g., $\text{Cu}^I\text{Br}/\text{Me}_6\text{TREN}$, $\text{Cu}^I\text{Br}/\text{Me}_6\text{TPMA}$, and also $\text{Cu}^I\text{Br}/\text{Cyclam-B}$ are the three most active complexes in Figure 2. This may be associated with a small entropic penalty in ligand rearrangement from Cu^I to Cu^{II} state.⁶³ Cyclic ligands are located in the middle of the scale, indicating normal activities when

- (34) Haddleton, D. M.; Clark, A. J.; Crossman, M. C.; Duncalf, D. J.; Heming, A. M.; Morsley, S. R.; Shooter, A. J. *Chem. Commun.* **1997**, 1173.
- (35) Queffelec, J.; Gaynor, S. G.; Matyjaszewski, K. *Macromolecules* **2000**, *33*, 8629–8639.
- (36) Inoue, Y.; Matyjaszewski, K. *Macromolecules* **2004**, *37*, 4014–4021.
- (37) Zeng, F.; Shen, Y.; Zhu, S.; Pelton, R. *Macromolecules* **2000**, *33*, 1628–1635.
- (38) Golub, G.; Cohen, H.; Paoletti, P.; Bencini, A.; Messori, L.; Bertini, I.; Meyerstein, D. *J. Am. Chem. Soc.* **1995**, *117*, 8353.
- (39) Wong, E. H.; Weisman, G. R.; Hill, D. C.; Reed, D. P.; Rogers, M. E.; Condon, J. S.; Fagan, M. A.; Calabrese, J. C.; Lam, K.-C.; Guzei, I. A.; Rheingold, A. L. *J. Am. Chem. Soc.* **2000**, *122*, 10561–10572.
- (40) Xia, J.; Zhang, X.; Matyjaszewski, K. *ACS Symp. Ser.* **2000**, *760* (Transition Metal Catalysis in Macromolecular Design), 207–223.
- (41) Qiu, J.; Shipp, D.; Gaynor, S. G.; Matyjaszewski, K. *Polym. Prepr. (Am. Chem. Soc., Div. Polym. Chem.)* **1999**, *40*, 418–419.
- (42) Matyjaszewski, K.; Patten, T. E.; Xia, J. *J. Am. Chem. Soc.* **1997**, *119*, 674–680.
- (43) Kickelbick, G.; Matyjaszewski, K. *Macromol. Rapid Commun.* **1999**, *20*, 341–346.
- (44) Xia, J.; Matyjaszewski, K. *Macromolecules* **1999**, *32*, 2434–2437.
- (45) Tang, H.; Radosz, M.; Shen, Y. *Polym. Prepr. (Am. Chem. Soc., Div. Polym. Chem.)* **2006**, *47* (1), 156–157.
- (46) Tang, H.; Radosz, M.; Shen, Y. *Polym. Prepr. (Am. Chem. Soc., Div. Polym. Chem.)* **2006**, *47* (1), 93–94.
- (47) Wulkow, M. *Macromol. Theor. Simul.* **1996**, *5*, 393–416.
- (48) Kothe, T.; Marque, S.; Martschke, R.; Popov, M.; Fischer, H. *J. Chem. Soc., Perkin Trans. 2* **1998**, 1553–1559.
- (49) Tang, W.; Tsarevsky, N. V.; Matyjaszewski, K. *J. Am. Chem. Soc.* **2006**, *128*, 1598–1604.
- (50) Ding, S.; Shen, Y.; Radosz, M. *J. Polym. Sci., Part A: Polym. Chem.* **2004**, *42*, 3553–3562.
- (51) Gromada, J.; Spanswick, J.; Matyjaszewski, K. *Macromol. Chem. Phys.* **2004**, *205*, 551–566.
- (52) Teodorescu, M.; Matyjaszewski, K. *Macromolecules* **1999**, *32*, 4826–4831.
- (53) Wang, J.-S.; Matyjaszewski, K. *Macromolecules* **1995**, *28*, 7901–10.
- (54) Xia, J.; Matyjaszewski, K. *Macromolecules* **1997**, *30*, 7697–7700.
- (55) Rorabacher, D. B. *Chem. Rev.* **2004**, *104*, 651–697.
- (56) Wang, J.-S.; Matyjaszewski, K. *J. Am. Chem. Soc.* **1995**, *117*, 5614–15.
- (57) Xia, J.; Gaynor, S. G.; Matyjaszewski, K. *Macromolecules* **1998**, *31*, 5958–5959.
- (58) Ambundo, E. A.; Deydier, M.-V.; Grall, A. J.; Agüera-Vega, N.; Dressel, L. T.; Cooper, T. H.; Heeg, M. J.; Ochrymowycz, L. A.; Rorabacher, D. B. *Inorg. Chem.* **1999**, *38*, 4233–4242.
- (59) Paik, H.-j.; Teodorescu, M.; Xia, J.; Matyjaszewski, K. *Macromolecules* **1999**, *32*, 7023–7031.
- (60) Birkelbach, F.; Winter, M.; Floerke, U.; Haupt, H.-J.; Butzlaff, C.; Lengen, M.; Bill, E.; Trautwein, A. X.; Wieghardt, K.; Chaudhuri, P. *Inorg. Chem.* **1994**, *33*, 3990–4001.
- (61) Pintauer, T.; McKenzie, B.; Matyjaszewski, K. *ACS Symp. Ser.* **2003**, *854* (Advances in Controlled/Living Radical Polymerization), 130–147.
- (62) Qiu, J.; Matyjaszewski, K.; Thouin, L.; Amatore, C. *Macromol. Chem. Phys.* **2000**, *201*, 1625–1631.
- (63) Pintauer, T.; Matyjaszewski, K. *Coord. Chem. Rev.* **2005**, *249*, 1155–1184.

MA0609634